

Superconductivity in Sr_2RuO_4 Mediated by Coulomb Scattering

Shigeru Koikegami* and Yoshiyuki Yoshida

*Japan Society for the Promotion of Science,
6-Ichibancho, Chiyoda-ku, Tokyo 102-8471, Japan*

Takashi Yanagisawa

Nanoelectronics Research Institute, AIST Tsukuba Central 2, Tsukuba 305-8568, Japan

(Dated: today)

Abstract

We investigate the superconductivity in Sr_2RuO_4 on the basis of the three-dimensional three-band Hubbard model. We propose a model with Coulomb interactions among the electrons on the nearest-neighbor Ru sites. In our model the intersite Coulomb repulsion and exchange coupling can work as the effective interaction for the spin-triplet pairing. This effective interaction is enhanced by the band hybridization, which is mediated by the interlayer transfers. We investigate the possibility of this mechanism in the ground state and find that the orbital dependent spin-triplet superconductivity is more stable than the spin-singlet one for realistic parameters. This spin-triplet superconducting state has horizontal line nodes on the Fermi surface.

PACS numbers: 74.20.Fg, 74.20.Mn, 74.20.Rp

I. INTRODUCTION

The nature of the superconductivity in Sr_2RuO_4 has drawn much attention since its discovery in 1994.^{1,2} A lot of experiments have provided evidence that the superconductivity is unconventional. For instance, the superconductivity is extremely sensitive to the non-magnetic impurity scattering in contrast to Anderson's theorem on a conventional superconductor.³ Miyake and Narikiyo have successfully shown that such an anomalous effect of impurity in Sr_2RuO_4 can be explained as an evidence of the spin-triplet pairing superconductivity.⁴ Nuclear magnetic resonance (NMR) measurement has revealed that the ^{17}O Knight shift is almost unchanged in the transition into the superconducting phase.⁵ Furthermore, muon spin relaxation (μSR) time measurement⁶ and polarized-neutron scattering study⁷ clarified that in the superconducting phase the time reversal symmetry is broken. From these experimental evidences it is almost confirmed that the superconductivity in Sr_2RuO_4 is the spin-triplet superconductivity. In the past few years, the momentum dependence of the superconducting gap function has become the central issue of this spin-triplet superconductor. In Sr_2RuO_4 the Fermi surface consists of three cylindrical pieces mainly originated from the four Ru-4d electrons in three t_{2g} orbitals.^{8,9,10} Agterberg *et al.* insisted that the temperature dependences of specific heat, penetration depth, and thermal conductivity can be explained by the orbital dependent superconductivity.¹¹ Additionally, recent specific-heat measurement at low temperature suggests the existence of line nodes.¹²

In order to determine the location of the nodes, we need the experimental results obtained by directional probes. In Sr_2RuO_4 the magnetothermal conductivity measurement seems the most powerful tool to investigate the location of the nodes.^{13,14} Two groups have reported that the thermal conductivity has no notable anisotropy when the magnetic field is applied to the direction parallel to the conducting plane. These results are quite different from the result of the cuprate superconductor, and they suggest that the pairing state with vertical line nodes has less possibility for the candidate in Sr_2RuO_4 . Thus the pairing state with horizontal line nodes seems to be appropriate to explain these experimental results for Sr_2RuO_4 .

Since Sr_2RuO_4 has single-layered perovskite structure as in the case for $\text{La}_{2-x}\text{Sr}_x\text{CuO}_4$, it has been supposed that its superconductivity is mediated by largely enhanced fluctuations common to these two-dimensional materials.^{15,16,17,18,19} However, it seems difficult to explain

the spin-triplet pairing state with horizontal line node. In order to solve this problem, Hasegawa *et al.* listed the possible odd-parity states on the basis of the group-theoretical analysis.²⁰ In their analysis they took notice of the body-centered-tetragonal lattice of Ru with lattice constants a and c . And they insisted that in order to stabilize the gap function with the horizontal line node the effective interaction for electrons at \mathbf{r} and $\mathbf{r} \pm (a/2)\hat{\mathbf{x}} \pm (a/2)\hat{\mathbf{y}} \pm (c/2)\hat{\mathbf{z}}$ is crucial. Zhitomirsky and Rice have successfully shown that the gap function with the horizontal line node may lead to the temperature dependence of the specific heat observed in experiments.²¹ Furthermore, Annett *et al.* have reproduced the experimental data of the superfluid density and the thermal conductivity on the basis of the multiband attractive Hubbard model with interlayer coupling.²²

In this paper we propose that the superconductivity in Sr_2RuO_4 is mediated by Coulomb scatterings among the electrons at \mathbf{r} and $\mathbf{r} \pm (a/2)\hat{\mathbf{x}} \pm (a/2)\hat{\mathbf{y}} \pm (c/2)\hat{\mathbf{z}}$. Our model Hamiltonian is the three-dimensional (3D) three-band Hubbard model with quasi-two-dimensional character. Our microscopic description of the superconductivity in Sr_2RuO_4 may be considered as an application of the two-band mechanism superconductivity to the spin-triplet Cooper pairing,²³ or as the three-dimensional version of the spin-triplet superconductivity in the one-dimensional chain with long-range attractive Coulomb interactions.²⁴

II. 3D THREE-BAND HUBBARD MODEL

We consider three t_{2g} orbitals of Ru-4d electron, i.e., d_{xy} , d_{yz} , and d_{zx} , in our 3D three-band Hubbard model. It is represented in real space as

$$\begin{aligned}
H = & \sum_{\mathbf{r}\mathbf{r}'\varphi\varphi'\sigma} [\varepsilon_\varphi \delta_{\mathbf{r}\mathbf{r}'} \delta_{\varphi\varphi'} - t_{\varphi\varphi'}(\mathbf{r}, \mathbf{r}')] c_{\varphi\mathbf{r}\sigma}^\dagger c_{\varphi'\mathbf{r}'\sigma} \\
& + \sum_{\mathbf{r}\mathbf{r}'\varphi\varphi'\sigma\sigma'} U_{\varphi\varphi'}^{\sigma\sigma'}(\mathbf{r}, \mathbf{r}') c_{\varphi\mathbf{r}\sigma}^\dagger c_{\varphi'\mathbf{r}'\sigma'}^\dagger c_{\varphi'\mathbf{r}'\sigma'} c_{\varphi\mathbf{r}\sigma} \\
& + \sum_{\mathbf{r}\mathbf{r}'\varphi\varphi'\sigma\sigma'} J_{\varphi\varphi'}^{\sigma\sigma'}(\mathbf{r}, \mathbf{r}') c_{\varphi\mathbf{r}\sigma}^\dagger c_{\varphi'\mathbf{r}'\sigma'}^\dagger c_{\varphi'\mathbf{r}'\sigma'} c_{\varphi\mathbf{r}\sigma} \\
& + \sum_{\mathbf{r}\mathbf{r}'\varphi\varphi'\sigma\sigma'} K_{\varphi\varphi'}^{\sigma\sigma'}(\mathbf{r}, \mathbf{r}') c_{\varphi\mathbf{r}\sigma}^\dagger c_{\varphi'\mathbf{r}'\sigma'}^\dagger c_{\varphi'\mathbf{r}'\sigma'} c_{\varphi\mathbf{r}\sigma}, \tag{1}
\end{aligned}$$

where $c_{\varphi\mathbf{r}\sigma}$ ($c_{\varphi\mathbf{r}\sigma}^\dagger$) is the annihilation (creation) operator of d electron with orbital $\varphi = \{xy, yz, zx\}$ and spin $\sigma = \{\uparrow, \downarrow\}$ on site \mathbf{r} . ε_φ are site energies, as we set $\varepsilon_{zx(yz)} = \Delta > 0$ and $\varepsilon_{xy} = 0$. $t_{\varphi\varphi'}(\mathbf{r}, \mathbf{r}')$ are hopping integrals, as set

$$t_{zx\,zx}(\mathbf{r}, \mathbf{r} \pm a\hat{\mathbf{x}}) = t_{yz\,yz}(\mathbf{r}, \mathbf{r} \pm a\hat{\mathbf{y}}) = t_0, \tag{2}$$

$$t_{zxzx}(\mathbf{r}, \mathbf{r} \pm a\hat{\mathbf{y}}) = t_{yzyz}(\mathbf{r}, \mathbf{r} \pm a\hat{\mathbf{x}}) = t_1, \quad (3)$$

$$\begin{aligned} & t_{zx yz (yz zx)}(\mathbf{r}, \mathbf{r} \pm a\hat{\mathbf{x}} + a\hat{\mathbf{y}}) \\ &= -t_{zx yz (yz zx)}(\mathbf{r}, \mathbf{r} \pm a\hat{\mathbf{x}} - a\hat{\mathbf{y}}) = \pm t_2, \end{aligned} \quad (4)$$

$$t_{xyxy}(\mathbf{r}, \mathbf{r} \pm a\hat{\mathbf{x}}) = t_{xyxy}(\mathbf{r}, \mathbf{r} \pm a\hat{\mathbf{y}}) = t_3, \quad (5)$$

$$t_{xyxy}(\mathbf{r}, \mathbf{r} \pm a\hat{\mathbf{x}} \pm a\hat{\mathbf{y}}) = t_4, \quad (6)$$

$$t_{zxzx (yz yz)}\left(\mathbf{r}, \mathbf{r} \pm \frac{a}{2}\hat{\mathbf{x}} \pm \frac{a}{2}\hat{\mathbf{y}} \pm \frac{c}{2}\hat{\mathbf{z}}\right) = t'_\perp, \quad (7)$$

and

$$\begin{aligned} & t_{zxxy (xy zx)}\left(\mathbf{r}, \mathbf{r} \pm \frac{a}{2}\hat{\mathbf{x}} + \frac{a}{2}\hat{\mathbf{y}} + \frac{c}{2}\hat{\mathbf{z}}\right) \\ &= t_{zxxy (xy zx)}\left(\mathbf{r}, \mathbf{r} \pm \frac{a}{2}\hat{\mathbf{x}} - \frac{a}{2}\hat{\mathbf{y}} - \frac{c}{2}\hat{\mathbf{z}}\right) \\ &= -t_{zxxy (xy zx)}\left(\mathbf{r}, \mathbf{r} \pm \frac{a}{2}\hat{\mathbf{x}} + \frac{a}{2}\hat{\mathbf{y}} - \frac{c}{2}\hat{\mathbf{z}}\right) \\ &= -t_{zxxy (xy zx)}\left(\mathbf{r}, \mathbf{r} \pm \frac{a}{2}\hat{\mathbf{x}} - \frac{a}{2}\hat{\mathbf{y}} + \frac{c}{2}\hat{\mathbf{z}}\right) \\ &= t_{yzxy (xy yz)}\left(\mathbf{r}, \mathbf{r} + \frac{a}{2}\hat{\mathbf{x}} \pm \frac{a}{2}\hat{\mathbf{y}} + \frac{c}{2}\hat{\mathbf{z}}\right) \\ &= t_{yzxy (xy yz)}\left(\mathbf{r}, \mathbf{r} - \frac{a}{2}\hat{\mathbf{x}} \pm \frac{a}{2}\hat{\mathbf{y}} - \frac{c}{2}\hat{\mathbf{z}}\right) \\ &= -t_{yzxy (xy yz)}\left(\mathbf{r}, \mathbf{r} + \frac{a}{2}\hat{\mathbf{x}} \pm \frac{a}{2}\hat{\mathbf{y}} - \frac{c}{2}\hat{\mathbf{z}}\right) \\ &= -t_{yzxy (xy yz)}\left(\mathbf{r}, \mathbf{r} - \frac{a}{2}\hat{\mathbf{x}} \pm \frac{a}{2}\hat{\mathbf{y}} + \frac{c}{2}\hat{\mathbf{z}}\right) \\ &= t''_\perp. \end{aligned} \quad (8)$$

Hereafter, we only consider the on-site interactions and the interactions among the nearest neighbors along the c axis, because the interactions among the nearest neighbors on the conduction ab plane are negligible due to screening. If we take $\{\hat{\mathbf{r}}_i\}_{i=1,\dots,8} = \{[\pm(a/2)\hat{\mathbf{x}}, \pm(a/2)\hat{\mathbf{y}}, \pm(c/2)\hat{\mathbf{z}}]\}$, the Coulomb integrals in Eq. (1) turn out

$$U_{\varphi\varphi'}^{\sigma\sigma'}(\mathbf{r}, \mathbf{r}') = U_{\varphi\varphi'}^0(1 - \delta_{\varphi\varphi'}\delta_{\sigma\sigma'})\delta_{\mathbf{r}\mathbf{r}'} + U_{\varphi\varphi'}^1 \sum_{i=1}^8 \delta_{\mathbf{r}\mathbf{r}'+\hat{\mathbf{r}}_i}, \quad (9)$$

$$J_{\varphi\varphi'}^{\sigma\sigma'}(\mathbf{r}, \mathbf{r}') = J_{\varphi\varphi'}^0(1 - \delta_{\varphi\varphi'})\delta_{\mathbf{r}\mathbf{r}'} + J_{\varphi\varphi'}^1 \sum_{i=1}^8 \delta_{\mathbf{r}\mathbf{r}'+\hat{\mathbf{r}}_i}, \quad (10)$$

$$K_{\varphi\varphi'}^{\sigma\sigma'}(\mathbf{r}, \mathbf{r}') = \left(K_{\varphi\varphi'}^0(1 - \delta_{\varphi\varphi'})\delta_{\mathbf{r}\mathbf{r}'} + K_{\varphi\varphi'}^1 \sum_{i=1}^8 \delta_{\mathbf{r}\mathbf{r}'+\hat{\mathbf{r}}_i} \right) \delta_{\sigma-\sigma'}, \quad (11)$$

where $U_{\varphi\varphi'}$, $J_{\varphi\varphi'}$, and $K_{\varphi\varphi'}$ are Coulomb repulsions, exchange interactions, and pair hoppings, respectively. Then we transform our Hamiltonian from the representation in real

space into the one in momentum \mathbf{k} space by Fourier transform, and decompose it into $H = H_0 + H'$. The noninteracting part H_0 is represented by

$$H_0 = \sum_{\mathbf{k}\sigma} \left(c_{zx\mathbf{k}\sigma}^\dagger c_{yz\mathbf{k}\sigma}^\dagger c_{xy\mathbf{k}\sigma}^\dagger \right) \begin{pmatrix} \varepsilon_{zx\mathbf{k}} + t_{\perp\mathbf{k}}^1 & t_{\parallel\mathbf{k}} & t_{\perp\mathbf{k}}^2 \\ t_{\parallel\mathbf{k}} & \varepsilon_{yz\mathbf{k}} + t_{\perp\mathbf{k}}^1 & t_{\perp\mathbf{k}}^3 \\ t_{\perp\mathbf{k}}^2 & t_{\perp\mathbf{k}}^3 & \varepsilon_{xy\mathbf{k}} \end{pmatrix} \begin{pmatrix} c_{zx\mathbf{k}\sigma} \\ c_{yz\mathbf{k}\sigma} \\ c_{xy\mathbf{k}\sigma} \end{pmatrix}. \quad (12)$$

In Eq. (12) we denote

$$\varepsilon_{zx\mathbf{k}} = \Delta - 2t_0 \cos k_x - 2t_1 \cos k_y, \quad (13)$$

$$\varepsilon_{yz\mathbf{k}} = \Delta - 2t_0 \cos k_y - 2t_1 \cos k_x, \quad (14)$$

$$\varepsilon_{xy\mathbf{k}} = -2t_3(\cos k_x + \cos k_y) - 4t_4 \cos k_x \cos k_y, \quad (15)$$

$$t_{\perp\mathbf{k}}^1 = -8t'_\perp \cos \frac{k_x}{2} \cos \frac{k_y}{2} \cos \frac{k_z c}{2}, \quad (16)$$

$$t_{\perp\mathbf{k}}^2 = 8t''_\perp \cos \frac{k_x}{2} \sin \frac{k_y}{2} \sin \frac{k_z c}{2}, \quad (17)$$

$$t_{\perp\mathbf{k}}^3 = 8t''_\perp \cos \frac{k_y}{2} \sin \frac{k_x}{2} \sin \frac{k_z c}{2}, \quad (18)$$

and $t_{\parallel\mathbf{k}} = -4t_2 \sin k_x \sin k_y$, taking the in-plane lattice constant as unity. We can diagonalize H_0 with respect to the band indices $\zeta = \{\alpha, \beta, \gamma\}$ as $H_0 = \sum_{\mathbf{k}\sigma} \sum_{\zeta} \varepsilon_{\zeta\mathbf{k}} a_{\zeta\mathbf{k}\sigma}^\dagger a_{\zeta\mathbf{k}\sigma}$ by orthogonal transformations, $c_{\varphi\mathbf{k}\sigma}^\dagger = \sum_{\zeta} R_{\zeta\varphi\mathbf{k}} a_{\zeta\mathbf{k}\sigma}^\dagger$ and $c_{\varphi\mathbf{k}\sigma} = \sum_{\zeta} R_{\varphi\zeta\mathbf{k}} a_{\zeta\mathbf{k}\sigma}$. The interacting part H' is represented by

$$\begin{aligned} H' = & \frac{1}{N} \sum_{\mathbf{k}\mathbf{k}'\mathbf{q}} \sum_{\sigma\sigma'} \sum_{\varphi\varphi'} U_{\varphi\varphi'}^0 (1 - \delta_{\varphi\varphi'} \delta_{\sigma\sigma'}) c_{\varphi\mathbf{k}+\mathbf{q}\sigma}^\dagger c_{\varphi'\mathbf{k}'-\mathbf{q}\sigma'}^\dagger c_{\varphi'\mathbf{k}'\sigma'} c_{\varphi\mathbf{k}\sigma} \\ & + \frac{1}{N} \sum_{\mathbf{k}\mathbf{k}'\mathbf{q}} \sum_{\sigma\sigma'} \sum_{\varphi\varphi'} J_{\varphi\varphi'}^0 (1 - \delta_{\varphi\varphi'}) c_{\varphi\mathbf{k}+\mathbf{q}\sigma}^\dagger c_{\varphi'\mathbf{k}'-\mathbf{q}\sigma'}^\dagger c_{\varphi\mathbf{k}'\sigma'} c_{\varphi'\mathbf{k}\sigma} \\ & + \frac{1}{N} \sum_{\mathbf{k}\mathbf{k}'\mathbf{q}} \sum_{\sigma\sigma'} \sum_{\varphi\varphi'} K_{\varphi\varphi'}^0 (1 - \delta_{\varphi\varphi'}) \delta_{\sigma-\sigma'} c_{\varphi\mathbf{k}+\mathbf{q}\sigma}^\dagger c_{\varphi\mathbf{k}'-\mathbf{q}\sigma'}^\dagger c_{\varphi'\mathbf{k}'\sigma'} c_{\varphi'\mathbf{k}\sigma} \\ & + \frac{1}{N} \sum_{\mathbf{k}\mathbf{k}'\mathbf{q}} \sum_{\sigma\sigma'} \sum_{\varphi\varphi'} \left[U_{\varphi\varphi'\mathbf{q}}^1 c_{\varphi\mathbf{k}+\mathbf{q}\sigma}^\dagger c_{\varphi'\mathbf{k}'-\mathbf{q}\sigma'}^\dagger c_{\varphi'\mathbf{k}'\sigma'} c_{\varphi\mathbf{k}\sigma} + J_{\varphi\varphi'\mathbf{q}}^1 c_{\varphi\mathbf{k}+\mathbf{q}\sigma}^\dagger c_{\varphi'\mathbf{k}'-\mathbf{q}\sigma'}^\dagger c_{\varphi\mathbf{k}'\sigma'} c_{\varphi'\mathbf{k}\sigma} \right] \\ & + \frac{1}{N} \sum_{\mathbf{k}\mathbf{k}'\mathbf{q}} \sum_{\sigma\sigma'} \sum_{\varphi\varphi'} K_{\varphi\varphi'\mathbf{q}}^1 \delta_{\sigma-\sigma'} c_{\varphi\mathbf{k}+\mathbf{q}\sigma}^\dagger c_{\varphi\mathbf{k}'-\mathbf{q}\sigma'}^\dagger c_{\varphi'\mathbf{k}'\sigma'} c_{\varphi'\mathbf{k}\sigma}, \end{aligned} \quad (19)$$

where N is the number of \mathbf{k} -space points in the first Brillouin zone (FBZ), and

$$U_{\varphi\varphi'\mathbf{q}}^1 = 8U_{\varphi\varphi'}^1 \cos \frac{q_x}{2} \cos \frac{q_y}{2} \cos \frac{q_z c}{2}, \quad (20)$$

$$J_{\varphi\varphi'\mathbf{q}}^1 = 8J_{\varphi\varphi'}^1 \cos \frac{q_x}{2} \cos \frac{q_y}{2} \cos \frac{q_z C}{2}, \quad (21)$$

$$K_{\varphi\varphi'\mathbf{q}}^1 = 8K_{\varphi\varphi'}^1 \cos \frac{q_x}{2} \cos \frac{q_y}{2} \cos \frac{q_z C}{2}. \quad (22)$$

III. SPIN-TRIPLET SUPERCONDUCTIVITY

For our model we get a self-consistency equation for a gap function of the ζ band, $\Delta_{\zeta\mathbf{k}}$, within the weak-coupling formalism:

$$\Delta_{\zeta\mathbf{k}} = -\frac{1}{2} \sum_{\mathbf{k}'\zeta'} V_{\zeta\zeta'\mathbf{k}\mathbf{k}'} \frac{\Delta_{\zeta'\mathbf{k}'}}{\sqrt{(\varepsilon_{\zeta'\mathbf{k}'} - \mu)^2 + |\Delta_{\zeta'\mathbf{k}'}|^2}}, \quad (23)$$

where μ is the chemical potential. Since our model does not include any asymmetrical interactions for spin state, e.g., spin-orbit interaction, this self-consistency equation is applicable to both spin-singlet and spin-triplet pairs in similar ways. For example, when we apply Eq. (23) to a spin-triplet pair taking its odd parity, i.e., $\Delta_{\zeta-\mathbf{k}} = -\Delta_{\zeta\mathbf{k}}$, into account, we get the expression of $V_{\zeta\zeta'}$ as below:

$$V_{\zeta\zeta'\mathbf{k}\mathbf{k}'} = \frac{2}{N} \sum_{\varphi\varphi'} \left[R_{\varphi\zeta\mathbf{k}} R_{\varphi'\zeta'\mathbf{k}'} U_{\varphi\varphi'\mathbf{k}-\mathbf{k}'}^1 R_{\zeta'\varphi'\mathbf{k}} R_{\zeta'\varphi\mathbf{k}'} \right. \\ \left. + R_{\varphi\zeta\mathbf{k}} R_{\varphi'\zeta'\mathbf{k}'} J_{\varphi\varphi'\mathbf{k}-\mathbf{k}'}^1 R_{\zeta'\varphi\mathbf{k}} R_{\zeta'\varphi'\mathbf{k}'} \right]. \quad (24)$$

On the other hand, in the case for a spin-singlet pair, $V_{\zeta\zeta'}$ can be expressed as

$$V_{\zeta\zeta'\mathbf{k}\mathbf{k}'} = \frac{2}{N} \sum_{\varphi\varphi'} \left\{ R_{\varphi\zeta\mathbf{k}} R_{\varphi'\zeta'\mathbf{k}'} \left(U_{\varphi\varphi'}^0 + U_{\varphi\varphi'\mathbf{k}-\mathbf{k}'}^1 \right) R_{\zeta'\varphi'\mathbf{k}} R_{\zeta'\varphi\mathbf{k}'} \right. \\ \left. + R_{\varphi\zeta\mathbf{k}} R_{\varphi'\zeta'\mathbf{k}'} \left[J_{\varphi\varphi'}^0 (1 - \delta_{\varphi\varphi'}) + J_{\varphi\varphi'\mathbf{k}-\mathbf{k}'}^1 \right] R_{\zeta'\varphi\mathbf{k}} R_{\zeta'\varphi'\mathbf{k}'} \right. \\ \left. + R_{\varphi\zeta\mathbf{k}} R_{\varphi\zeta'\mathbf{k}'} \left[K_{\varphi\varphi'}^0 (1 - \delta_{\varphi\varphi'}) + K_{\varphi\varphi'\mathbf{k}-\mathbf{k}'}^1 \right] R_{\zeta'\varphi'\mathbf{k}} R_{\zeta'\varphi\mathbf{k}'} \right\}. \quad (25)$$

When the gap magnitude Δ_{sc} is small compared to band parameters, we can reduce Eq. (23) into

$$\Delta_{\zeta\mathbf{k}} = \ln \Delta_{\text{sc}} \sum_{\mathbf{k}'\zeta'} V_{\zeta\zeta'\mathbf{k}\mathbf{k}'} \delta(\varepsilon_{\zeta'\mathbf{k}'} - \mu) \Delta_{\zeta'\mathbf{k}'}, \quad (26)$$

according to the Kondo's argument.²⁵ We choose our tight-binding band parameters as in Table I, where we take t_0 as a unit of energy estimated as about 1eV. We choose them so that we can well reproduce the Fermi surface measured by the de Haas-van Alphen effect^{26,27,28} as shown in Fig. 1. Here we treat our tight-binding band parameters and Coulomb integrals as phenomenological ones. Thus it can be thought that our Fermi surface includes the band

t_0	t_1	t_2	t_3	t_4	t'_\perp	t''_\perp	$U_{\varphi\varphi'}^0$	$J_{\varphi\varphi'}^0$	$K_{\varphi\varphi'}^0$	$U_{\varphi\varphi'}^1$	$J_{\varphi\varphi'}^1$	$K_{\varphi\varphi'}^1$
1.00	0.12	0.04	1.00	0.38	0.01	0.03	2.00	1.00	1.00	0.10	0.10	0.10

TABLE I: Transfers and Coulomb interactions.

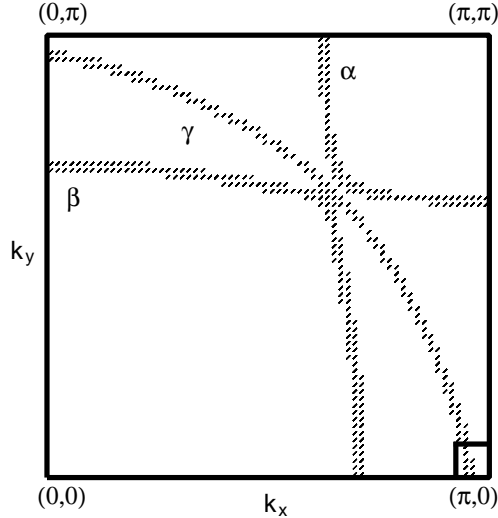


FIG. 1: Fermi surface in the case with $\Delta = 0.50$. Band indices α , β , and γ are indicated here.

renormalization effects due to the electron correlation, and that the Coulomb integrals are effective interactions reduced by Hartree-Fock decoupling. Hartree-Fock decoupling also affects on-site energies, which we can control by varying Δ . Our calculations are executed on equally spaced 256^3 \mathbf{k} points in FBZ for each band. When we take 224^3 \mathbf{k} points instead, our results of $\ln \Delta_{\text{sc}}$ vary less than 3%.

When we solve our reduced self-consistency equation (26), we find that the spin-triplet state is more stable than spin-singlet ones. One of this reason is that $U_{\varphi\varphi'\mathbf{k}-\mathbf{k}'}$ and $J_{\varphi\varphi'\mathbf{k}-\mathbf{k}'}$ in Eq. (24) can always change their signs due to their wave-vector dependences as shown in eqs. (20) and (21). Added to this, the band hybridization enhances the effective interaction of Eq. (24) via the matrix elements of orthogonal transformations, $R_{\varphi\zeta\mathbf{k}}$ and $R_{\zeta\varphi\mathbf{k}}$, in Eq. (24). As a result for these, $U_{\varphi\varphi'\mathbf{k}-\mathbf{k}'}$ and $J_{\varphi\varphi'\mathbf{k}-\mathbf{k}'}$ work like strong pair tunneling interactions among hybridized bands for spin-triplet pairing. As shown afterward, this hybridization is much important for our triplet superconductivity. One of the most stable pairing functions is

$$\Delta_{\zeta\mathbf{k}}^x = C_\zeta \sin \frac{k_x}{2} \cos \frac{k_y}{2} \cos \frac{k_z c}{2}, \quad (27)$$

where C_ζ is real and takes different value on each ζ band. Taking account of the spatial symmetry of our model, the other most stable function is

$$\Delta_{\zeta\mathbf{k}}^y = C_\zeta \sin \frac{k_y}{2} \cos \frac{k_x}{2} \cos \frac{k_z c}{2}. \quad (28)$$

It has indeed the same result of $\ln \Delta_{\text{sc}}$ as the function, Eq. (27). These pairing functions, Eqs. (27) and (28), have been proposed as candidates of the most stable state by Hasegawa *et al.*²⁰ In order to clarify the importance of the band hybridization, let us calculate the integrated effective matrix elements for our spin-triplet pairing function, Eq. (27),

$$v_{\zeta\zeta'} = \sum_{\mathbf{k}} ' \hat{\Delta}_{\zeta\mathbf{k}}^x \sum_{\mathbf{k}'} V_{\zeta\zeta'\mathbf{k}\mathbf{k}'} \delta(\varepsilon_{\zeta'\mathbf{k}'} - \mu) \hat{\Delta}_{\zeta'\mathbf{k}'}^x, \quad (29)$$

where $\sum_{\mathbf{k}} '$ denotes the momentum summation on the Fermi surface and $\hat{\Delta}_{\zeta\mathbf{k}}^x$ denotes the normalized function of (27) determined by

$$\sum_{\mathbf{k}} ' |\hat{\Delta}_{\zeta\mathbf{k}}^x|^2 = 1. \quad (30)$$

For example, when $\Delta = 0.50$, we obtain

$$\begin{pmatrix} v_{\alpha\alpha} & v_{\alpha\beta} & v_{\alpha\gamma} \\ v_{\beta\alpha} & v_{\beta\beta} & v_{\beta\gamma} \\ v_{\gamma\alpha} & v_{\gamma\beta} & v_{\gamma\gamma} \end{pmatrix} = \begin{pmatrix} 1.357 \times 10^{-3} & -1.175 \times 10^{-3} & -0.09952 \\ 0.1057 & 2.093 \times 10^{-3} & 1.074 \times 10^{-3} \\ 0.4129 \times 10^{-3} & 0.04082 & -2.015 \times 10^{-3} \end{pmatrix}. \quad (31)$$

Here, we can notice that the elements among the different bands $v_{\alpha\gamma}$, $v_{\gamma\beta}$, and $v_{\beta\alpha}$ have larger absolute values than the others. This is caused by the pair tunneling between the different bands, which is enhanced by the band hybridization. If we hope to increase our spin-triplet pairing instability, we should use these elements effectively. Judging from the inequalities, $v_{\alpha\gamma} < 0 < v_{\gamma\beta} < v_{\beta\alpha}$, if $C_\alpha \cdot C_\beta < 0$ and $C_\beta \cdot C_\gamma < 0$ and $C_\gamma \cdot C_\alpha > 0$, we expect that the eigenvalue of Eq. (26), $(\ln \Delta_{\text{sc}})^{-1}$, can take a large negative value for our gap function, Eq. (27). A large negative $(\ln \Delta_{\text{sc}})^{-1}$ results large Δ_{sc} . Indeed, our numerically obtained solution of C_ζ shown in Table II satisfy the above inequalities. Hence the pair tunneling enhanced by the band hybridization plays a significant role to realize our spin-triplet superconductivity.

Hereafter, we assume that the order parameter of spin-triplet superconductor with three components (d vector) is parallel to the z axis, $\mathbf{d}(\mathbf{k}) \propto \hat{z}(k_x + ik_y)$.²⁹ Then, we can reasonably construct our d vector as $d_z(\mathbf{k}) = \Delta_{\zeta\mathbf{k}}^x + i\Delta_{\zeta\mathbf{k}}^y$, which is a linear combination of our obtained

ζ	α	β	γ
C_ζ	0.1625	-0.1633	0.08613

TABLE II: C_ζ of Eq. (27) in the case with $\Delta = 0.50$.

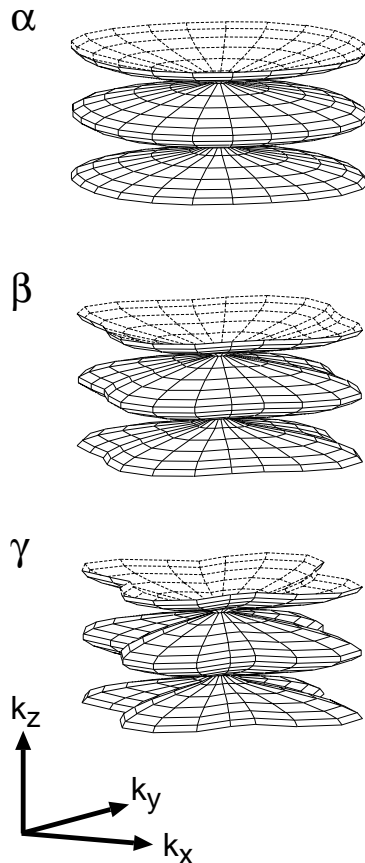


FIG. 2: Schematic pictures of gap amplitude on the Fermi surface of each band in the case with $\Delta = 0.50$. The amplitude of each band is normalized in convenience.

functions, Eqs. (27) and (28). We can show that the amplitude of d vector vary as $|d_z(\mathbf{k})| \propto \sqrt{1 - \cos k_x \cos k_y} |\cos(k_z c/2)|$, shown in Fig. 2. All of them have horizontal line nodes at $k_z = \pm\pi/c$ and fourfold symmetries around the c axis, and their amplitudes are larger along $[100]$ and $[010]$ than $[110]$. These results are qualitatively consistent with the magnetothermal conductivity measurements.^{13,14}

Then we study the Δ -dependence of $\ln \Delta_{sc}$. This result is shown in Fig. 3. We show only

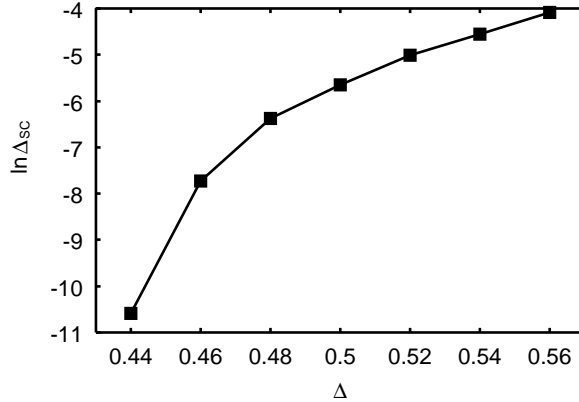


FIG. 3: Δ -dependence of $\ln \Delta_{sc}$.

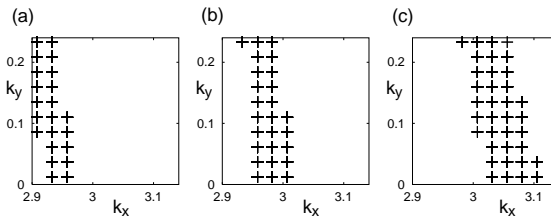


FIG. 4: Closeups of the Fermi surface projected on the plane with $k_z = 0$. (a), (b), and (c) are in the cases with $\Delta = 0.44$, 0.50 , and 0.56 , respectively. These areas are around the van Hove singular point as indicated in Fig. 1.

the case with $0.44 \leq \Delta \leq 0.56$ because in other cases $\ln \Delta_{sc}$ becomes extremely small. We can point out that our superconductivity is reinforced only when γ band has a large density of states. To make this situation clear, we magnify the part of Fermi surfaces and project it on the plane with $k_z = 0$. We show this part of all Fermi surfaces with different Δ in Fig. 4. The large density of states of the γ band can be realized when a piece of Fermi surface is close to the van Hove singular point $(\pi, 0)$. We have earlier shown that the pair tunneling enhanced by the band hybridization plays a significant role for our spin-triplet superconductivity. Thus our spin-triplet superconductivity needs the two important factors. It might be rare that both of these two factors present simultaneously in real materials. We can expect that in Sr_2RuO_4 both of these two conditions are wonderfully satisfied.

In our results Δ_{sc} can get to $e^{-4.084} \sim 16.8\text{meV}$. And, when a piece of the Fermi surface becomes closer to the van Hove singular point $(\pi, 0)$, Δ_{sc} will be much larger. These results are too much larger than the experimental results of Sr_2RuO_4 , estimated as $0.2 - 0.4\text{meV}$.

This may be caused by too large estimations of U^1 and J^1 . However, we think that this is mainly caused by the weak-coupling formalism and neglected quasiparticles' lifetime. If the strong correlation effect decreases the lifetime, we should take into account the retardation effect and then Δ_{sc} will be smaller. In Sr_2RuO_4 it is thought that the electrons correlate strongly with one another, and we should adopt the strong-coupling formalism for the quantitative estimation of Δ_{sc} .¹⁸ Although our quantitative estimation of Δ_{sc} has these problems, as far as the whole electrons in Sr_2RuO_4 compose the Fermi liquid, our obtained gap symmetry cannot be replaced by the other symmetries.

IV. CONCLUSION

In this paper, we demonstrated that the spin-triplet pairing mediated by the intersite Coulomb scatterings is more stable than the spin-singlet one in our model. The gap function has a fourfold symmetry and horizontal line nodes on the Fermi surface of each bands. These results appear qualitatively consistent with the experimental results. Therefore the interlayer Coulomb scatterings play a significant role in order to realize the spin-triplet superconductivity in Sr_2RuO_4 . Judged from the results about superconducting gap magnitude, our superconductivity is much sensitive to the band parameters. Our superconductivity is unique to the electronic state in Sr_2RuO_4 , which has both the degenerated orbitals and the interlayer transfers among these different orbitals.

Acknowledgments

The authors are grateful to J. Kondo, K. Yamaji, M. Sigrist, K. Izawa, I. Hase, N. Shirakawa, S. I. Ikeda, and S. Koike for their invaluable comments. The computation in this work was performed on IBM RS/6000-SP at TACC and VT-Alpha servers at NeRI in AIST.

* Present address: Nanoelectronics Research Institute, AIST Tsukuba Central 2, Tsukuba 305-8568, Japan; email address: shigeru.koikegami@aist.go.jp

- ¹ Y. Maeno, H. Hashimoto, K. Yoshida, S. Nishizaki, T. Fujita, J. G. Bednorz, and F. Lichtenberg, *Nature (London)* **372**, 532 (1994).
- ² Y. Maeno, T. M. Rice, and M. Sigrist, *Phys. Today* **54**, 42 (2001).
- ³ A. P. Mackenzie, R. K. W. Haselwimmer, A. W. Tyler, G. G. Lonzarich, Y. Mori, S. Nishizaki, and Y. Maeno, *Phys. Rev. Lett.* **80**, 161 (1998).
- ⁴ K. Miyake and O. Narikiyo, *Phys. Rev. Lett.* **83**, 1423 (1999).
- ⁵ K. Ishida, H. Mukuda, Y. Kitaoka, K. Asayama, Z. Q. Mao, Y. Mori, and Y. Maeno, *Nature (London)* **396**, 658 (1998).
- ⁶ G. M. Luke *et al.*, *Nature (London)* **394**, 558 (1998).
- ⁷ J. A. Duffy, S. M. Hayden, Y. Maeno, Z. Mao, J. Kulda, and G. J. McIntyre, *Phys. Rev. Lett.* **85**, 5412 (2000).
- ⁸ D. J. Singh, *Phys. Rev. B* **52**, 1358 (1995).
- ⁹ T. Oguchi, *Phys. Rev. B* **51**, 1385 (1995).
- ¹⁰ I. Hase and Y. Nishihara, *J. Phys. Soc. Jpn.* **86**, 2653 (1996).
- ¹¹ D. F. Agterberg, T. M. Rice, and M. Sigrist, *Phys. Rev. Lett.* **78**, 3374 (1997).
- ¹² S. Nishizaki, Y. Maeno, and Z. Q. Mao, *J. Phys. Soc. Jpn.* **69**, 572 (2000).
- ¹³ M. A. Tanatar, M. Suzuki, S. Nagai, Z. Q. Mao, Y. Maeno, and T. Ishiguro, *Phys. Rev. Lett.* **86**, 2649 (2001).
- ¹⁴ K. Izawa *et al.*, *Phys. Rev. Lett.* **86**, 2653 (2001).
- ¹⁵ I. I. Mazin and D. Singh, *Phys. Rev. Lett.* **79**, 733 (1997); **82**, 4324 (1999).
- ¹⁶ P. Monthoux and G. G. Lonzarich, *Phys. Rev. B* **59**, 14 598 (1999).
- ¹⁷ R. Arita, K. Kuroki, and H. Aoki, *Phys. Rev. B* **60**, 14 585 (1999).
- ¹⁸ T. Nomura and K. Yamada, *J. Phys. Soc. Jpn.* **69**, 3678 (2000); **71**, 404 (2002).
- ¹⁹ T. Takimoto, *Phys. Rev. B* **62**, R14 641 (2000).
- ²⁰ Y. Hasegawa, K. Machida, and M. Ozaki, *J. Phys. Soc. Jpn.* **69**, 336 (2000).
- ²¹ M. E. Zhitomirsky and T. M. Rice, *Phys. Rev. Lett.* **87**, 057 001 (2001).
- ²² J. F. Annett, G. Litak, B. L. Györfy, and K. I. Wysokiński, *Phys. Rev. B* **66**, 134 514 (2002).
- ²³ J. Kondo, *Prog. Theor. Phys.* **29**, 1 (1963); *J. Phys. Soc. Jpn.* **71**, 1353 (2002).
- ²⁴ A. A. Aligia and L. Arrachea, *Phys. Rev. B* **60**, 15 332 (1999).
- ²⁵ J. Kondo, *J. Phys. Soc. Jpn.* **70**, 808 (2001).
- ²⁶ A. P. Mackenzie, S. R. Julian, A. J. Diver, G. J. McMullan, M. P. Ray, G. G. Lonzarich,

- Y. Maeno, S. Nishizaki, and T. Fujita, Phys. Rev. Lett. **76**, 3786 (1996).
- ²⁷ Y. Yoshida *et al.*, J. Phys. Soc. Jpn. **68**, 9 (1999).
- ²⁸ C. Bergemann, S. R. Julian, A. P. Mackenzie, S. NishiZaki, and Y. Maeno, Phys. Rev. Lett. **84**, 2662 (2000).
- ²⁹ T. M. Rice and M. Sigrist, J. Phys.: Condens. Matter **7**, L643 (1995).